

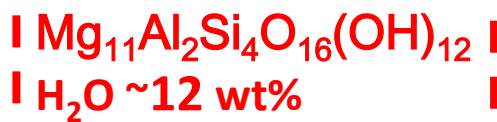
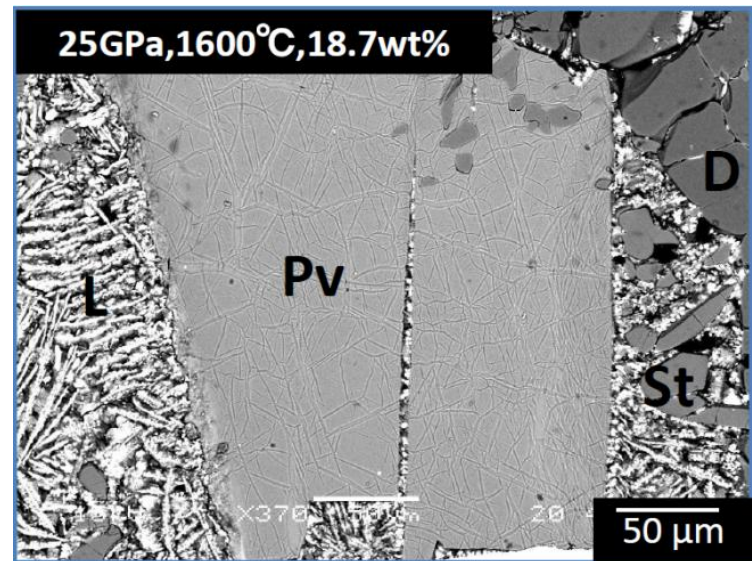
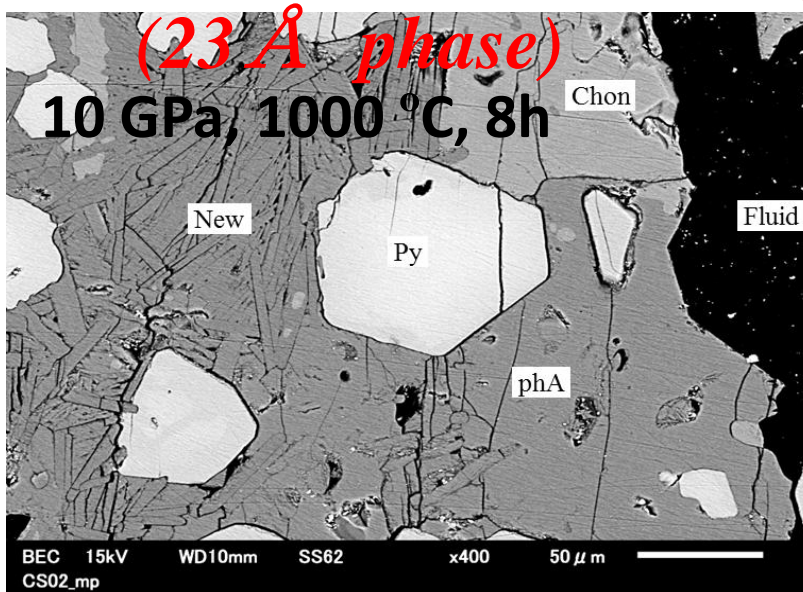
The stability and water solubility of high pressure hydrous and nominally anhydrous minerals in the mantle

Toru Inoue (GRC, Ehime Univ.)

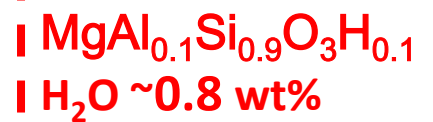
Collaborators: Sho Kakizawa¹, Nao Cai¹, Kiyoshi Fujino¹,
Takahiro Kuribayashi², Toshiro Nagase², Steeve Gréaux¹,
Yuji Higo³, Naoya Sakamoto⁴, Hisayoshi Yurimoto⁴

1 Ehime Univ., 2 Tohoku Univ., 3 JASRI, 4 Hokkaido Univ.

Aluminous new phase *hydrous bridgmanite (perovskite)*



Cai et al.
(2015)



Inoue et al.
(in prep.)

Discovery of **hydrous ringwoodite** in diamond inclusion

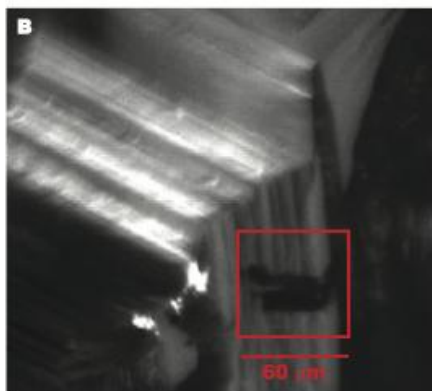
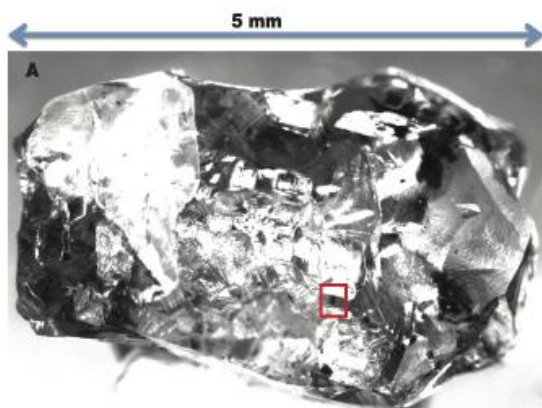
(Pearson et al., 2014)

LETTER

doi:10.1038/nature1308

Hydrous mantle transition zone indicated by ringwoodite included within diamond

D. G. Pearson¹, F. E. Brenker², F. Nestola³, J. McNeill⁴, L. Nasdala⁵, M. T. Hutchison⁶, S. Matveev¹, K. Mather⁴, G. Silversmit⁷, S. Schmitz², B. Vekemans⁷ & L. Vincze⁷



Discovery in diamond inclusion

~1.5 wt% H₂O included

The mantle transition zone is really hydrous condition, at least in some regions.

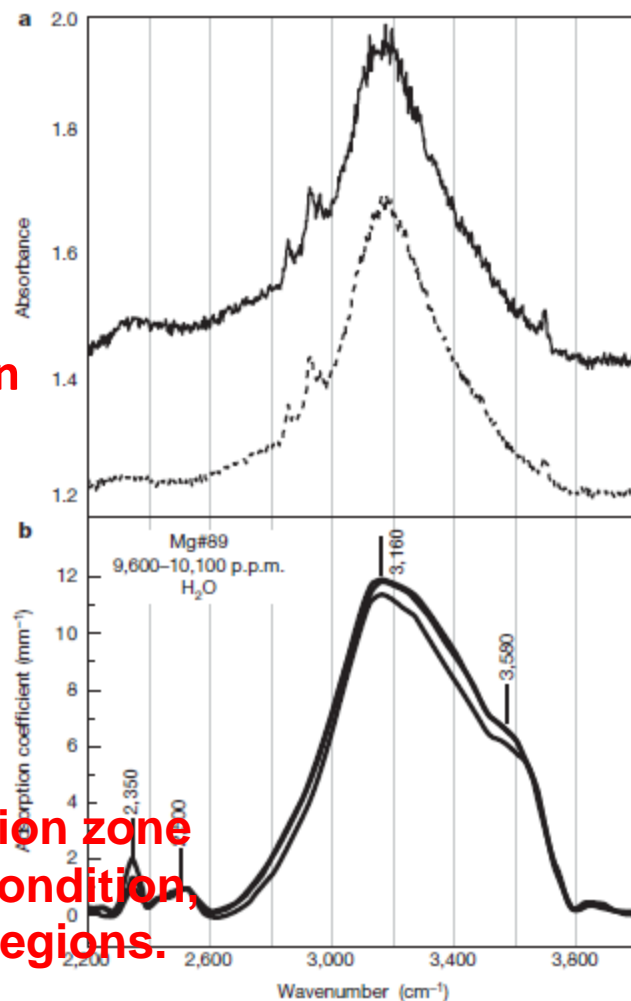
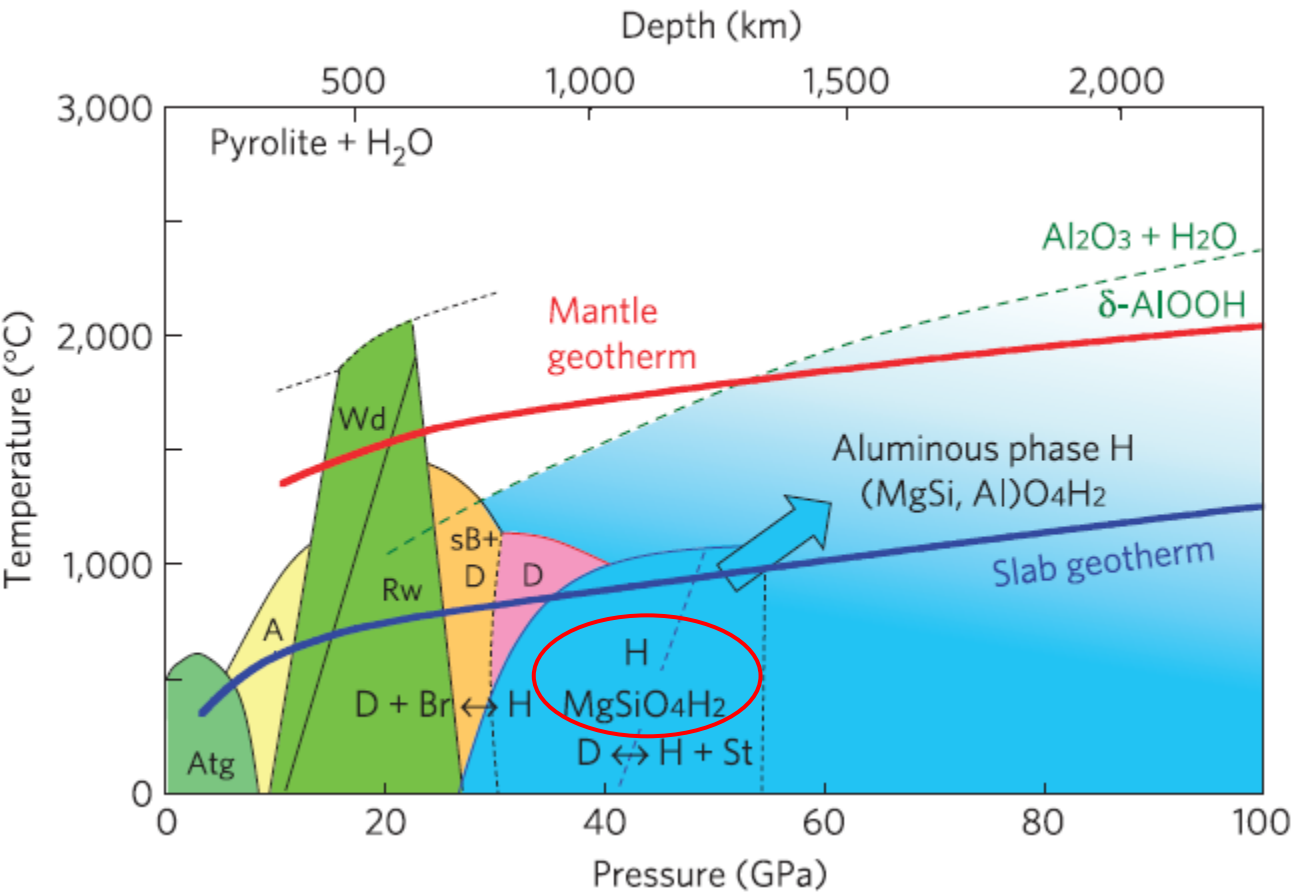


Figure 2 | FTIR spectra of ringwoodite inclusion in Juína diamond JUC29. **a**, Unpolarized FTIR spectra for ringwoodite inclusion in diamond JUC29 between 2,200 and 3,900 cm^{-1} . The two spectra were measured at $\sim 90^\circ$ degrees to each other and are unsmoothed, but were corrected for a background that includes the intrinsic response of the host diamond. Water contents calculated by integration of these two spectra are between 1.4 and 1.5 wt% (see Methods section on FTIR). **b**, Reference spectra for hydrous Fe-bearing ringwoodite (Mg# 89) containing ~ 1 wt% H_2O (ref. 27).

Extended Data Figure 1 | Image of JUC29 diamond and the ringwoodite-walstromite inclusion. **a**, Monochrome image of diamond JUC29 taken under incident light, with the ringwoodite-walstromite inclusion pair highlighted by a red square. The irregular shape and hexagonal pits in the

diamond are signs of significant resorption. **b**, Enlarged view of the area of the host diamond (rotated 90° relative to **a**) containing the ringwoodite-walstromite inclusion pair. The shadow behind the rectangular area outlining the inclusion pair is probably a stress fracture in the diamond.

Hydrous peridotite (MgO-SiO₂-H₂O system)



Mg₂SiO₄
Wd: wadsleyite
H₂O = ~3.3 wt%
Rw: ringwoodite
H₂O = ~2.5 wt%
SiO₂
St: stishovite

Nishi et al. (2014)

Atg: antigorite Mg₆Si₄O₁₀(OH)₈ H₂O = 13 wt%
A: phase A Mg₇Si₂H₆O₁₄ H₂O = 11.8 wt%
sB: superhydrous B Mg₁₀Si₃H₄O₁₈ H₂O = 5.8 wt%
D: phase D MgSi₂H₂O₆ H₂O = 10.1 wt%
H: phase H MgSiH₂O₄ H₂O = 15.2 wt%

Br: brucite Mg(OH)₂
 H₂O = 31 wt%
δ-AlOOH AlOOH
 H₂O = 15 wt%

Our group has been conducting the study for the stability and water solubility of hydrous and nominally anhydrous minerals, and *the recent target is the effect of Al, trivalent cation*. In this process, we found the *new Al-bearing hydrous phase (23 Å phase)* and *Al-bearing hydrous bridgmanite*.

Today's topic

- 1) Discovery of *new Al-bearing hydrous phase (23 Å phase)* stable *in upper mantle condition* (Cai et al., 2015)
- 2) Discovery of *Al-bearing hydrous bridgmanite* stable *in lower mantle condition* (Inoue et al., in prep.)

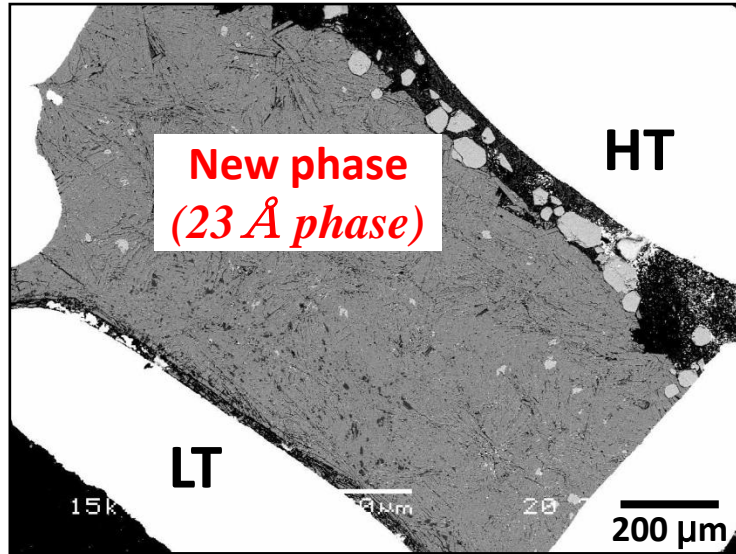
Al-bearing new hydrous phase
(23 Å phase)
in upper mantle condition

(Cai et al., 2015)

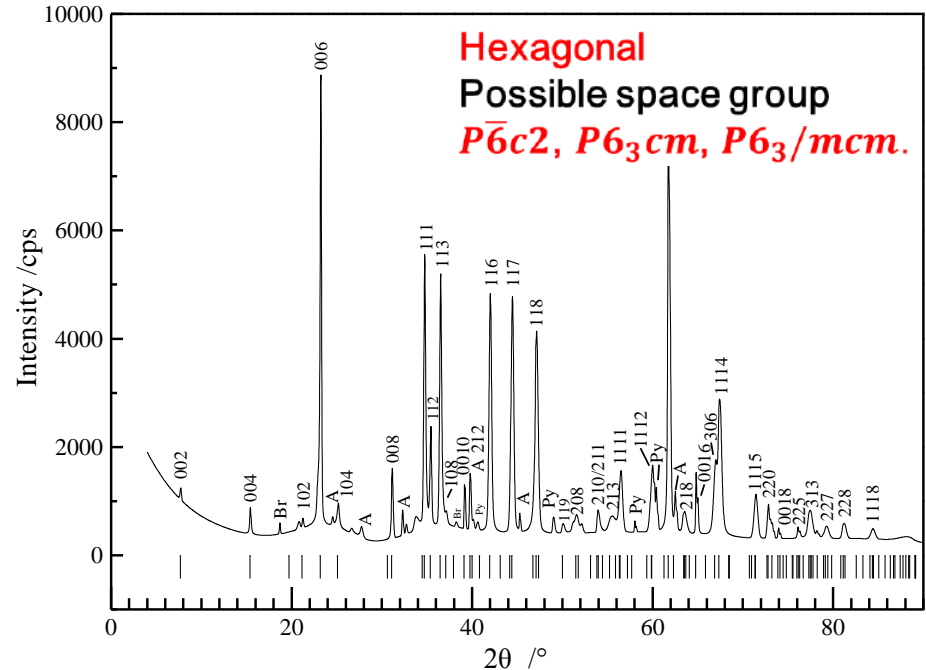
Al-bearing new hydrous phase (*23 Å phase*)

Starting composition: $\text{Mg}_{11}\text{Al}_2\text{Si}_4\text{O}_{15}(\text{OH})_{14}$

P&T: **10 GPa, 1000 °C**



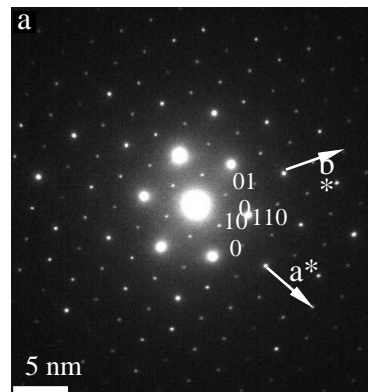
Fitting the XRD pattern by assuming a **hexagonal** structure



Chemical Composition (wt%)

MgO	Al ₂ O ₃	SiO ₂	H ₂ O	Total
49.84	11.75	26.46	11.95	100

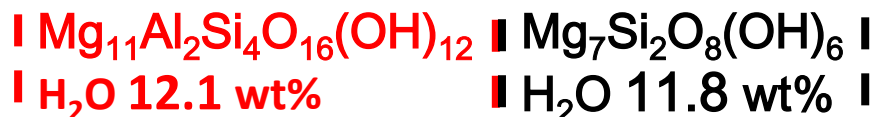
TEM observation



Lattice parameter

	new phase	phase A*
a	5.1972(9) Å	7.8603(2)
c	22.991(4) Å	9.5730(2)
V	537.8(2) Å³	512.22
ρ	2.760	2.959

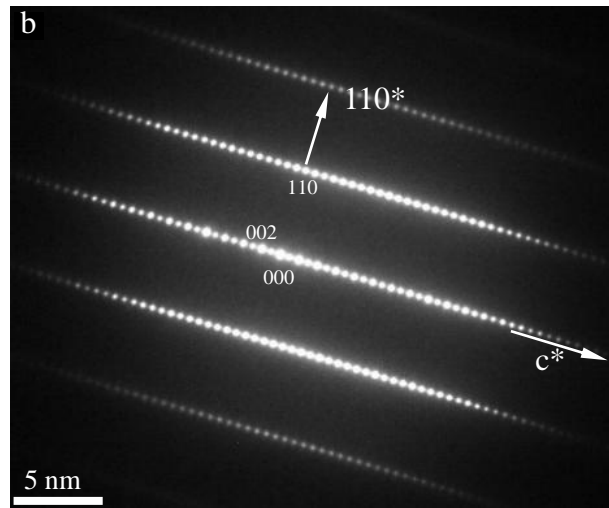
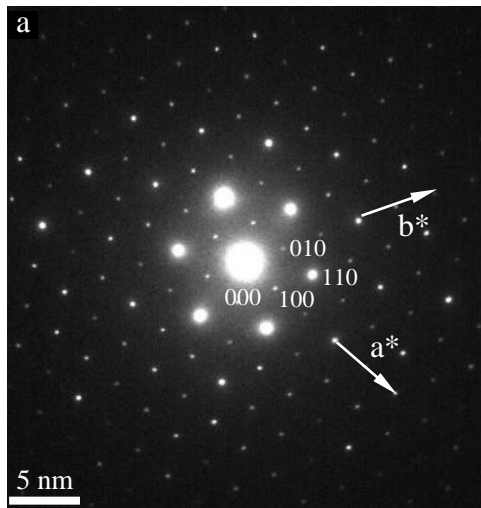
*Horiuchi et al., 1979



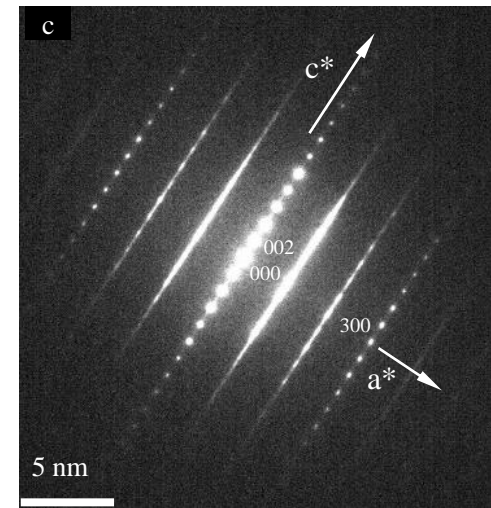
New phase
(23 Å phase)

phA

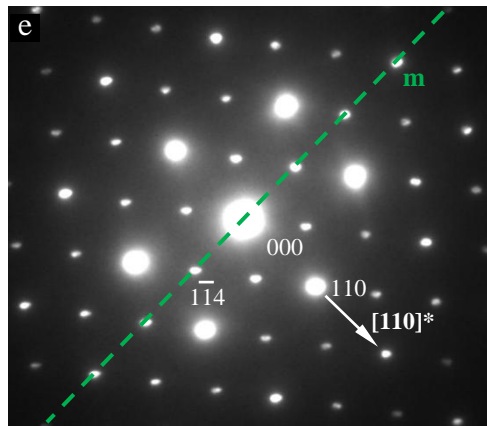
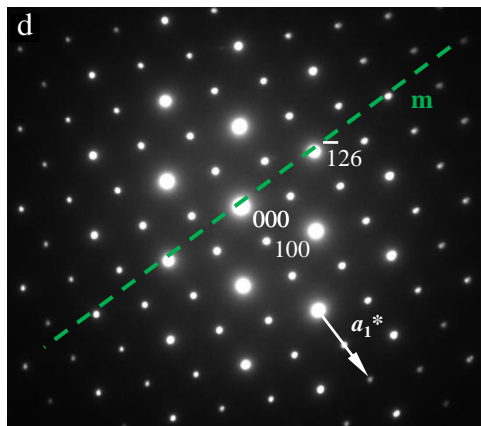
TEM observation



hhl spots



hhl spots



Mirror planes exist at every 30°.

- **Hexagonal** structure;
- *hhl* not extinct;
- *hhl* ($l = 2n+1$) extinct;
- $00l$ ($l = 2n+1$) extinct;
- **Mirror planes.**

Possible space group:
P6c2, *P63cm*, or *P63/mcm*

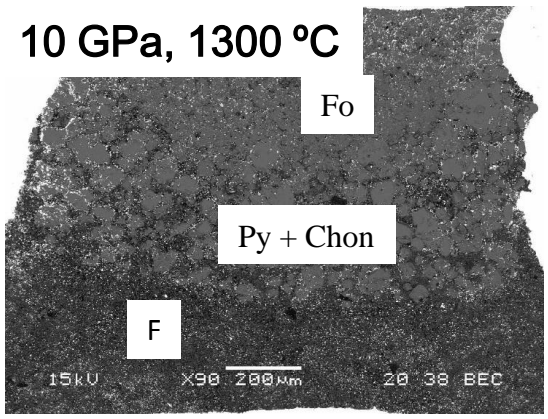
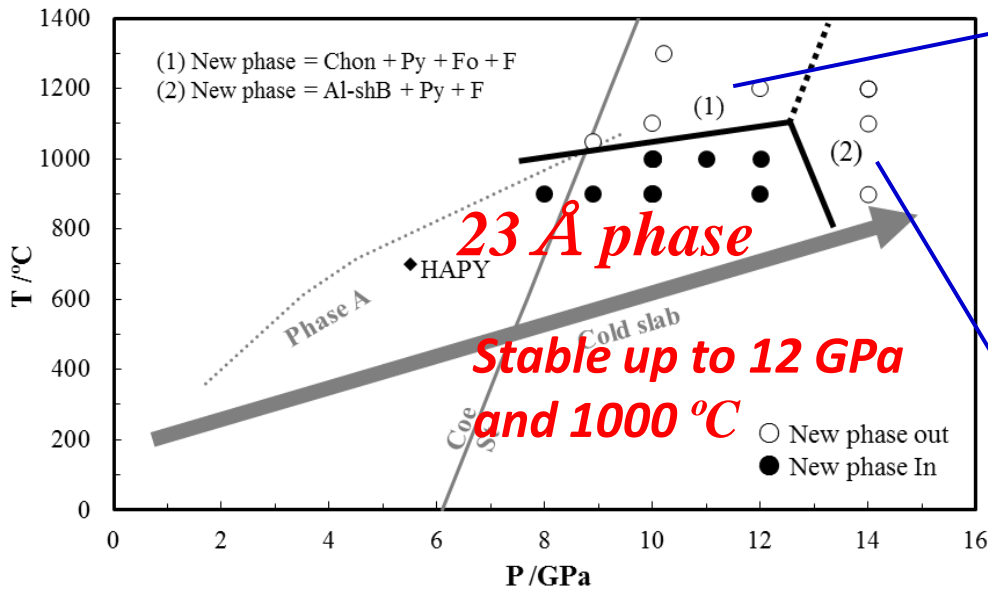
$a = 5.23(6) \text{ \AA}$, $c = 23.2(2) \text{ \AA}$

Stability region of *23 Å phase*

Break down:

<13 GPa

23 Å phase → Chon + Py + Fo + F



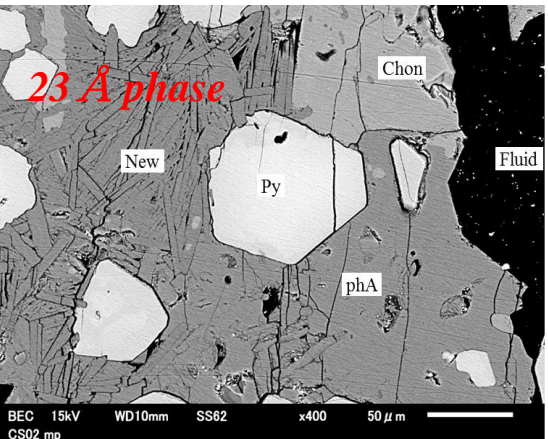
>13 GPa

23 Å phase → Al-shB + Py + F

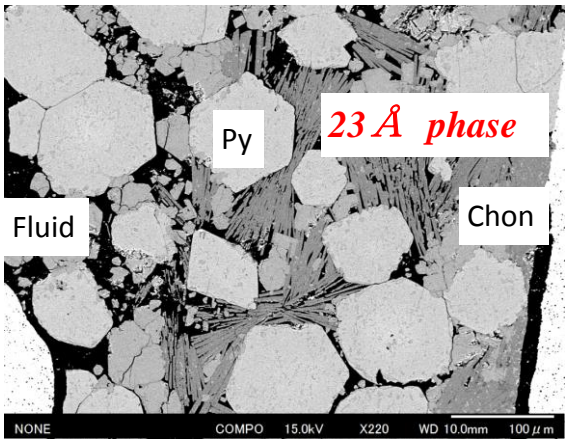
500 μm

23 Å phase is stable in Chlorite composition

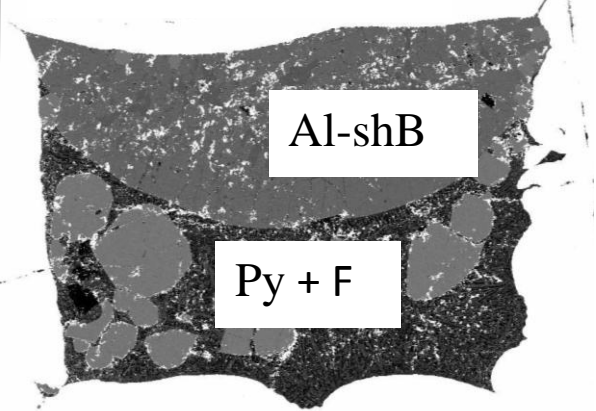
10 GPa, 1000 °C, 8h



7 GPa, 800 °C, 4h



14 GPa, 1200 °C



Fo: forsterite; Chon: chondrodite; Py: pyrope; Al-shB: Al-bearing superhydrous B; F: fluid

**Al-bearing hydrous bridgmanite
stable in lower mantle condition**

(Inoue et al., in prep.)

This PPT was modified from my oral presentation because before publication.

Chemical composition of Bridgmanite

Table. Chemical composition of Perovskite (mol)

P (GPa)	25	26	26
H ₂ O (wt%)	18.7	18.7	11.3
Mg	0.99	1	0.99
Al	0.09	0.09	0.11
Si	0.94	0.93	0.93
Cation sum	2.02	2.02	2.02
measured number	8	3	7

(T=1600°C)

Oxygen=3

No Mg deficit

Al incorporates into perovskite by the substitution of $Mg^{2+} + Si^{4+} \leftrightarrow 2Al^{3+}$ in anhydrous condition, but in hydrous condition, only Si deficit is observed.

Al-perovskite in DRY condition (1600°C)

25 GPa: $Mg_{0.96}Al_{0.08}Si_{0.96}O_3$

26 GPa: $Mg_{0.93}Al_{0.14}Si_{0.93}O_3$

DRY (Akaogi et al., 2002)

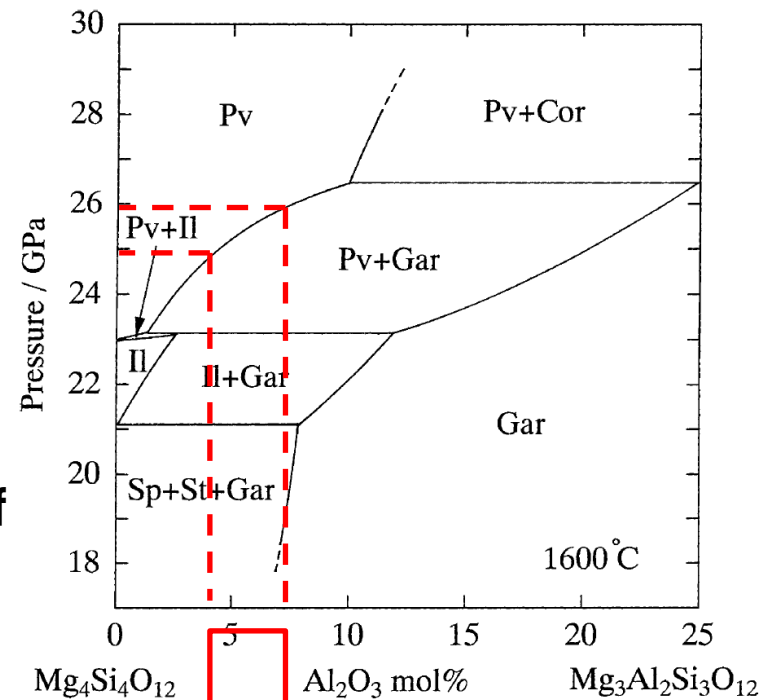
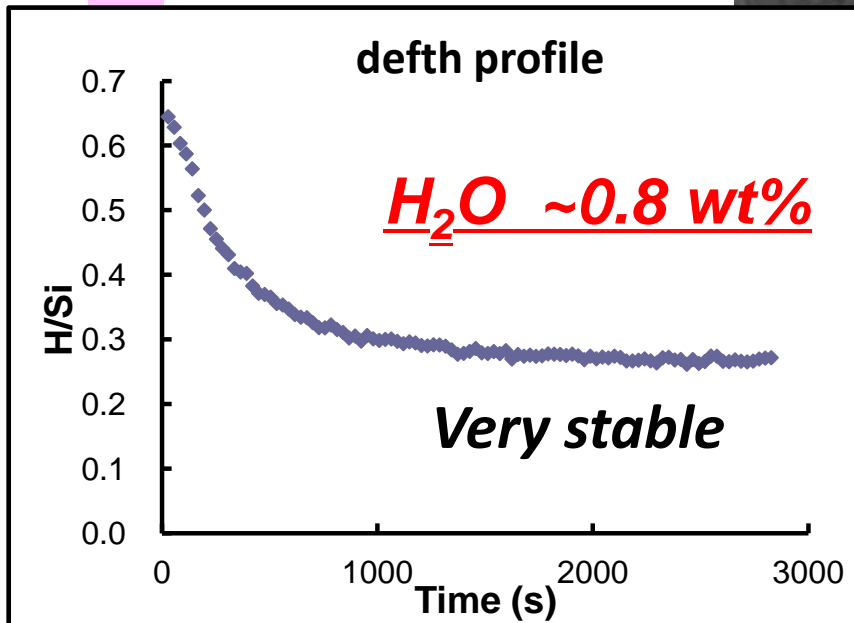
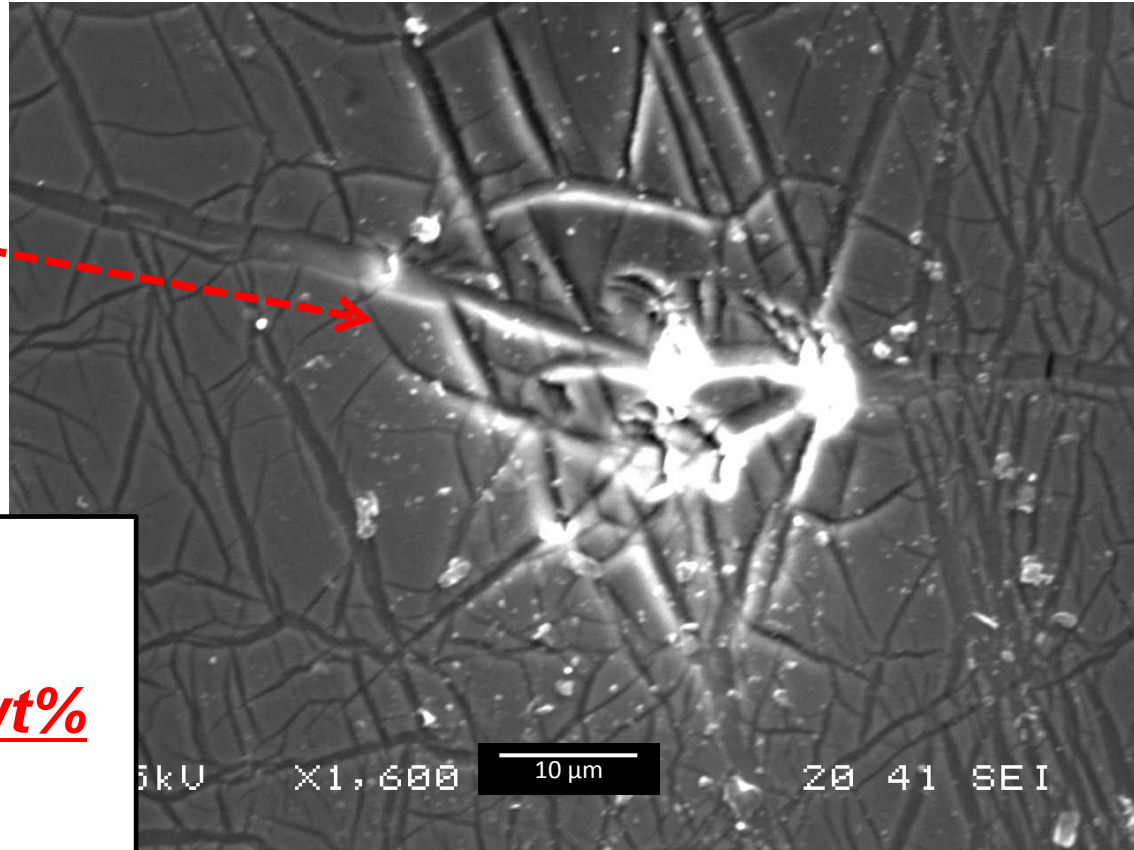
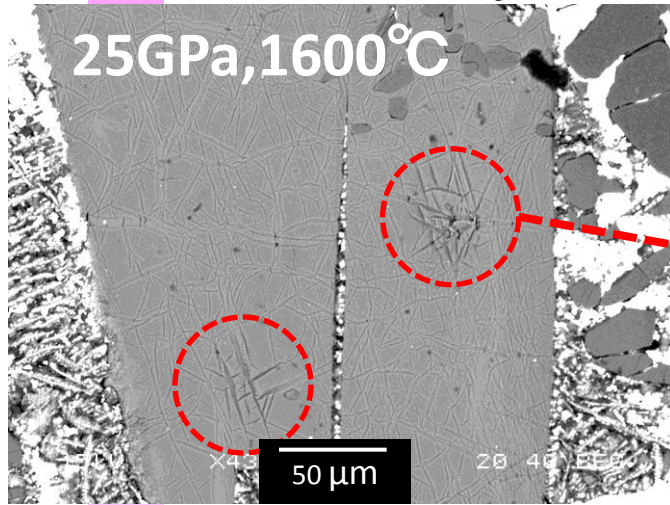


Fig. 3. Phase boundaries in the system $Mg_4Si_4O_{12}-Mg_3Al_2Si_3O_{12}$ at 1600°C up to 30 GPa determined by Kubo and Akaogi (2000). Abbreviations are the same as in Fig. 1.



H₂O measurement by SIMS

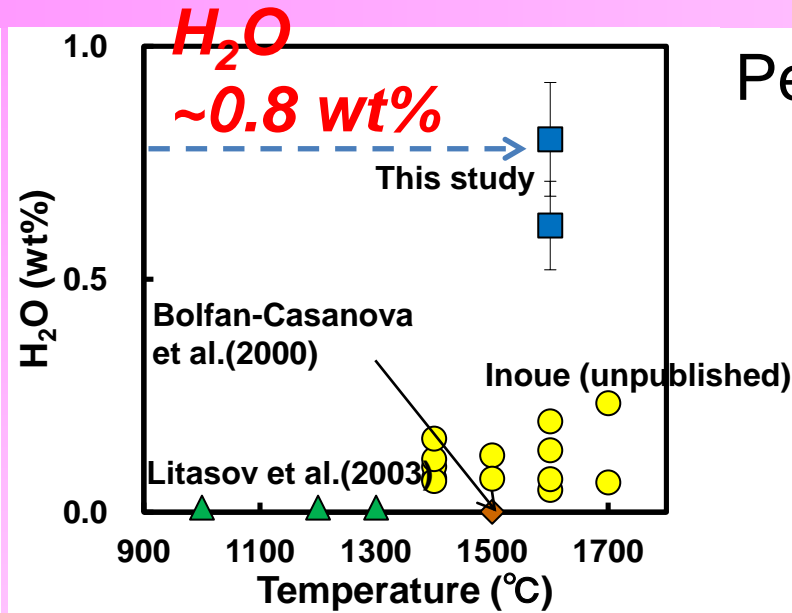
Hydrous bridgmanite



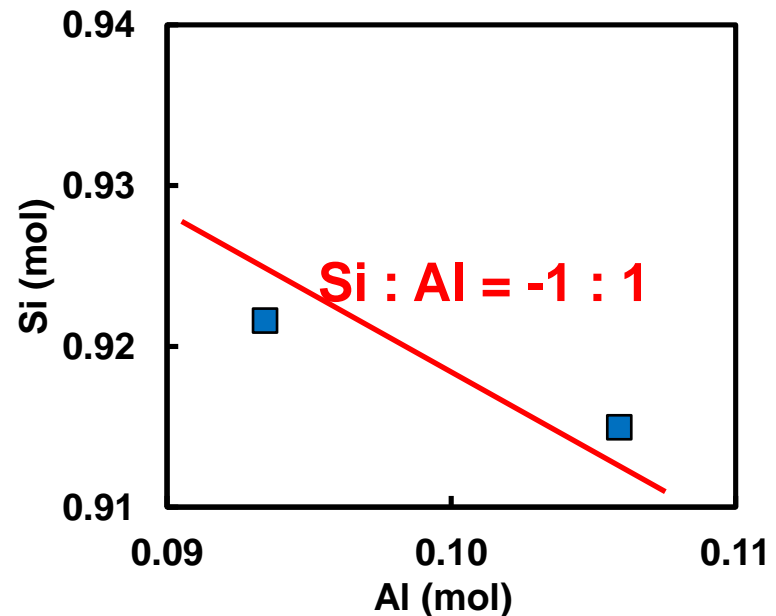
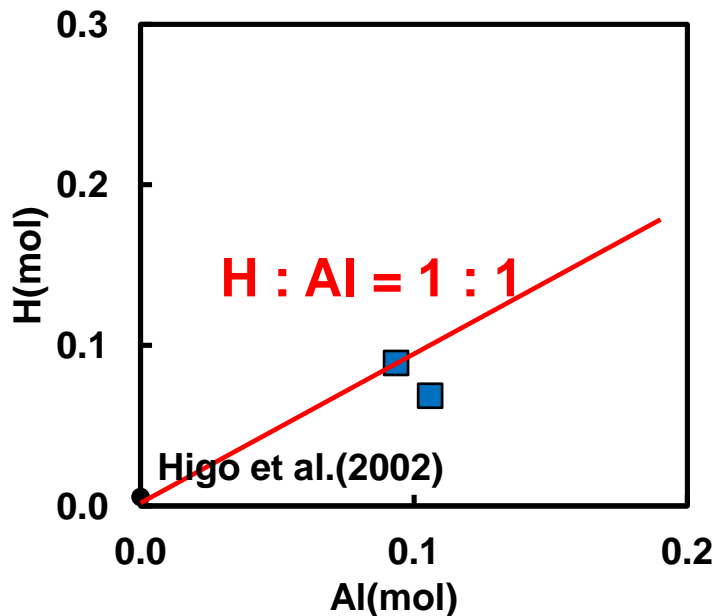
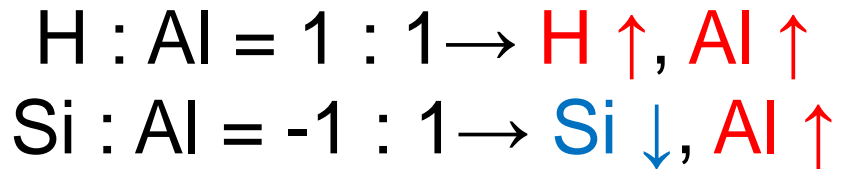
***Amphibole crystal (H₂O ~1.66 wt%)
was used as standard.***



perovskite(MgSiO_3) $\text{Mg}_{0.97}\text{Si}_{0.92}\text{Al}_{0.09}\text{H}_{0.09}\text{O}_3$



Perovskite includes Al_2O_3 ($\sim 5 \text{ wt}\%$)



Single crystal X-ray diffraction study

Automated four-circle diffractometer at BL-10A, PF, KEK

Structure refinement

- 1) SHELXL97 with WinGX software was used for all structural refinements (Scheldrick and Schneider 1997; Farrugia 1999).
- 2) Initial structural parameters of non-hydrogen atoms were taken from Horiuchi et al. (1987).
- 3) The averaged scattering values for dodecahedral (A) and octahedral (B) sites were modeled by the scattering factor of Mg^{2+} for A-site and that of Si^{4+} for B-site, respectively.
- 4) After the values were refined, the distributions of Mg, Al and Si at both A- and B-sites were evaluated by the optimization to minimize the summation of the squared residuals between the calculated and observed data such as the site scattering power (electron number) of each site, total amount of each atom in the unit cell, and the mean bond valence distance in each polyhedron within the restrictions of its bulk chemical formula.

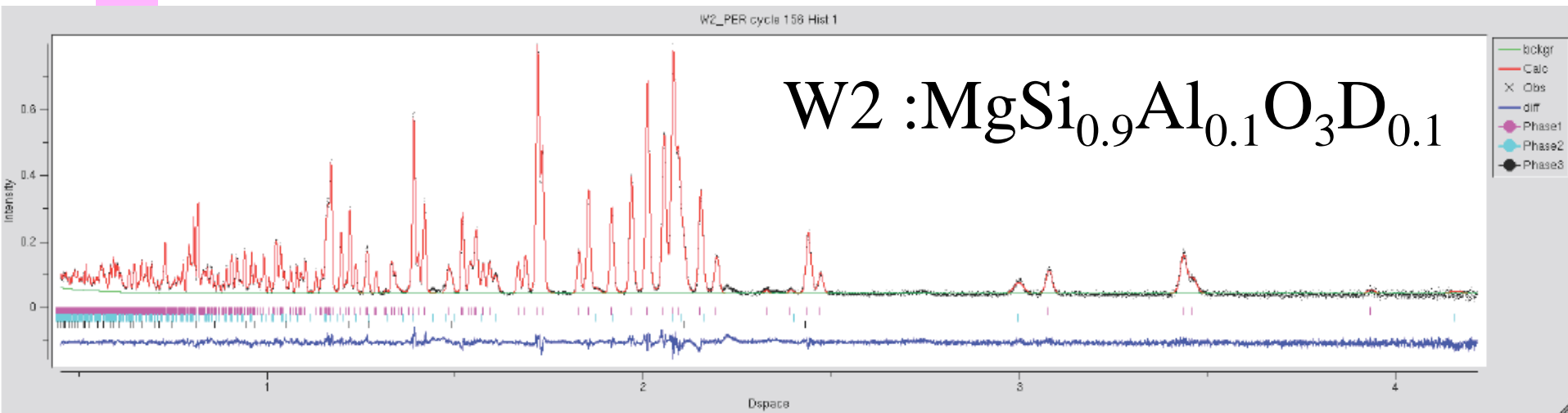


Rietveld analysis for neutron diffraction study

Slit size: 5 x 5 mm

Measurement time: 5 hr

Z-Rietveld program was used.

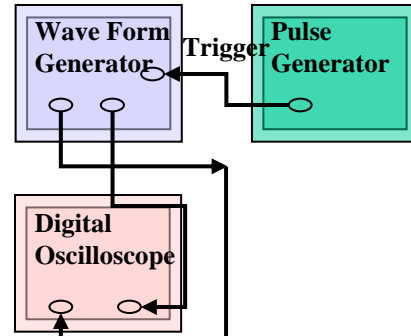


The above analysis was done by Pv : phase D: periclase = 90:8:2.
Still small amount of the other phase ($\delta\text{-AlOOH}$) may exist.

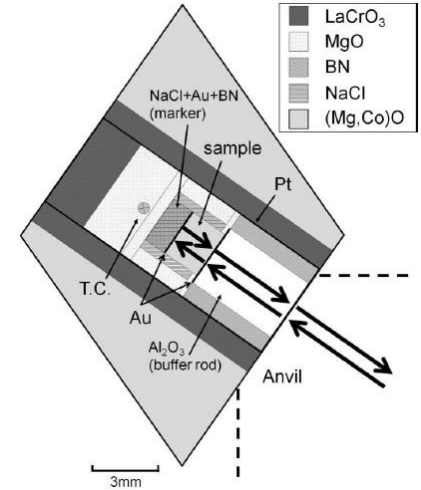
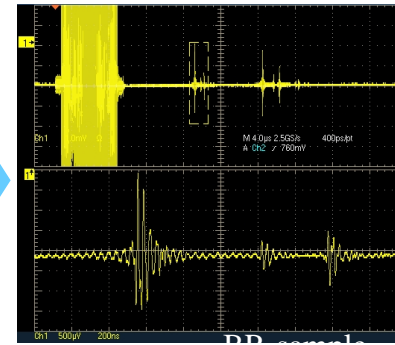


Sound velocity measurement under high P-T in SPring-8

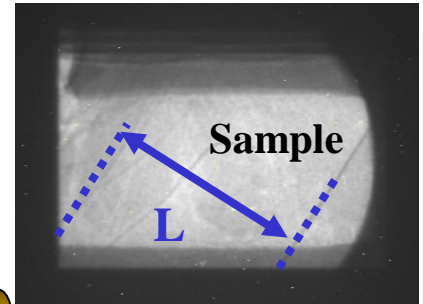
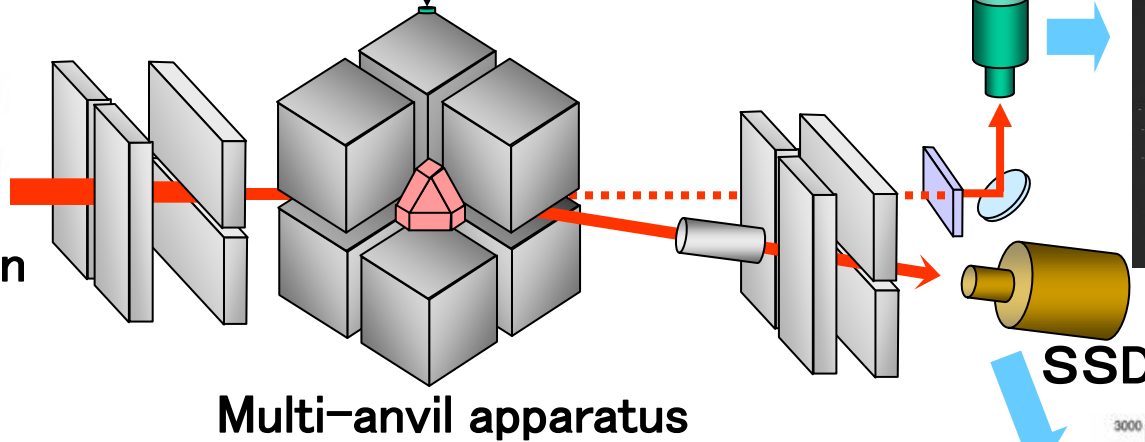
Sound velocity measurement system



travel time

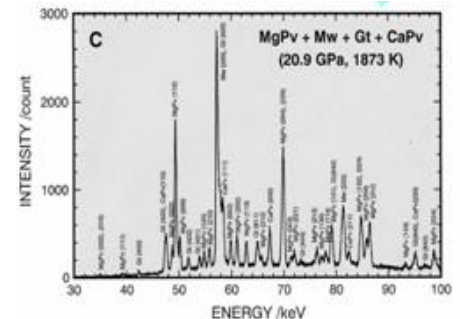


Synchrotron X-ray



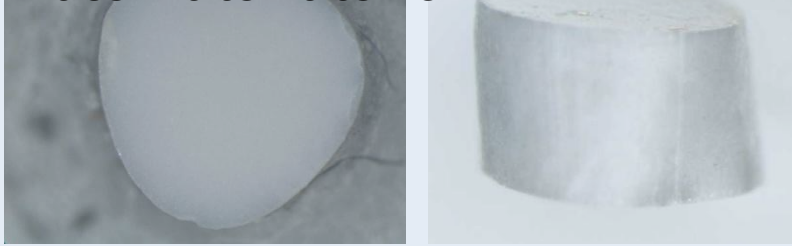
sample length

X-ray diffraction
(pressure, density,
phase identification)

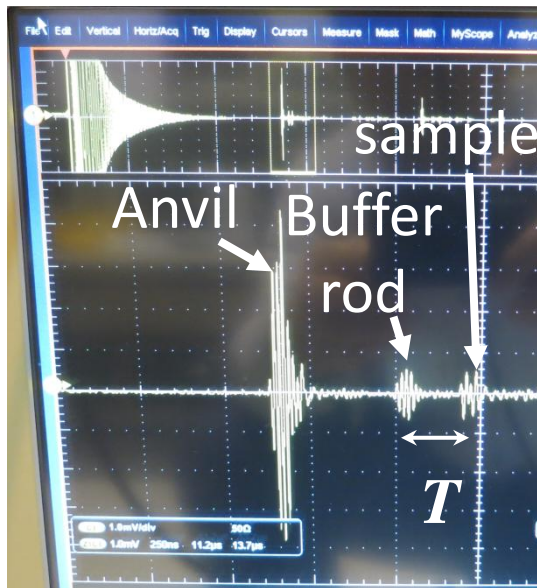
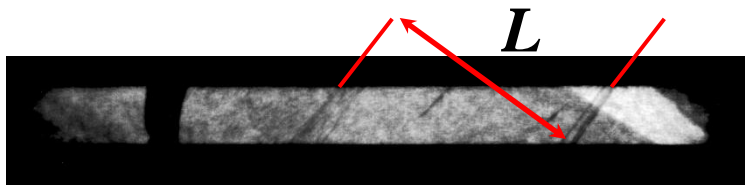


Ultrasonic velocity (V_p , V_s) measurement

hydrous bridgmanite:



2 mm



Sample length: L

Travel time: T

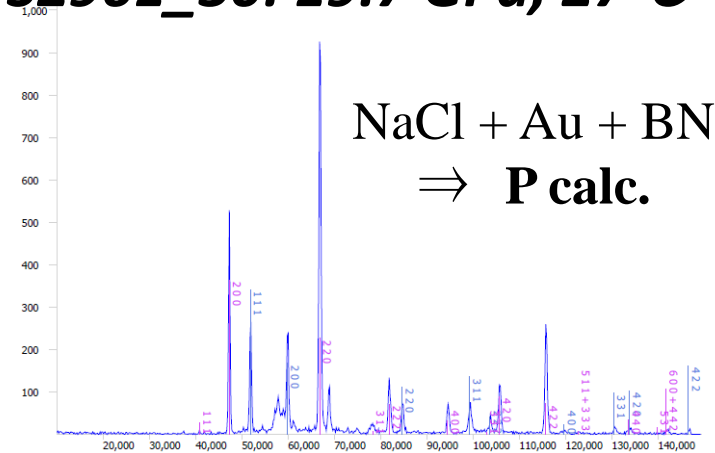
$\Rightarrow 2L/T$

$\Rightarrow V_p, V_s$

V_p : 60 MHz

V_s : 40 MHz

S2961_30: 19.7 GPa, 27°C

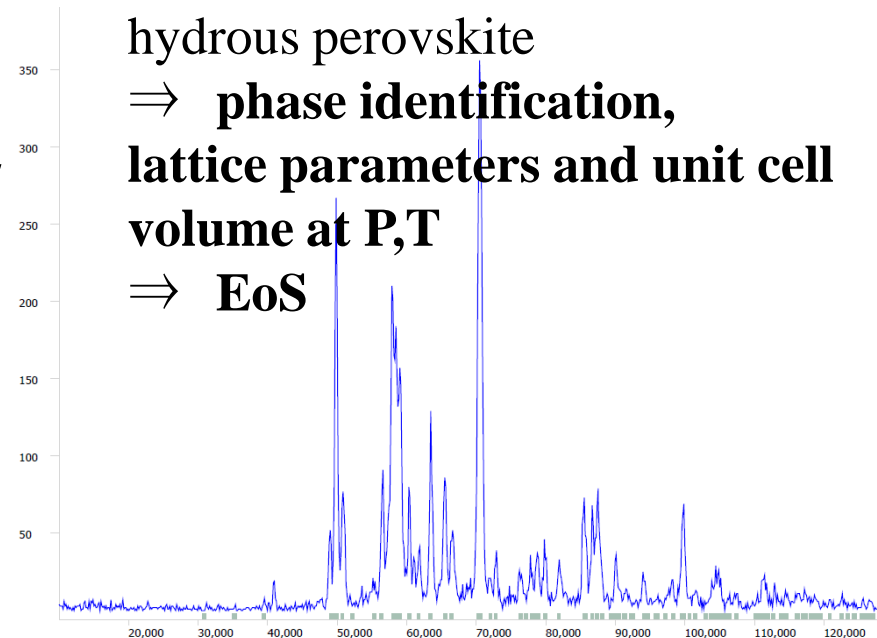


NaCl + Au + BN
 \Rightarrow **P calc.**

hydrous perovskite

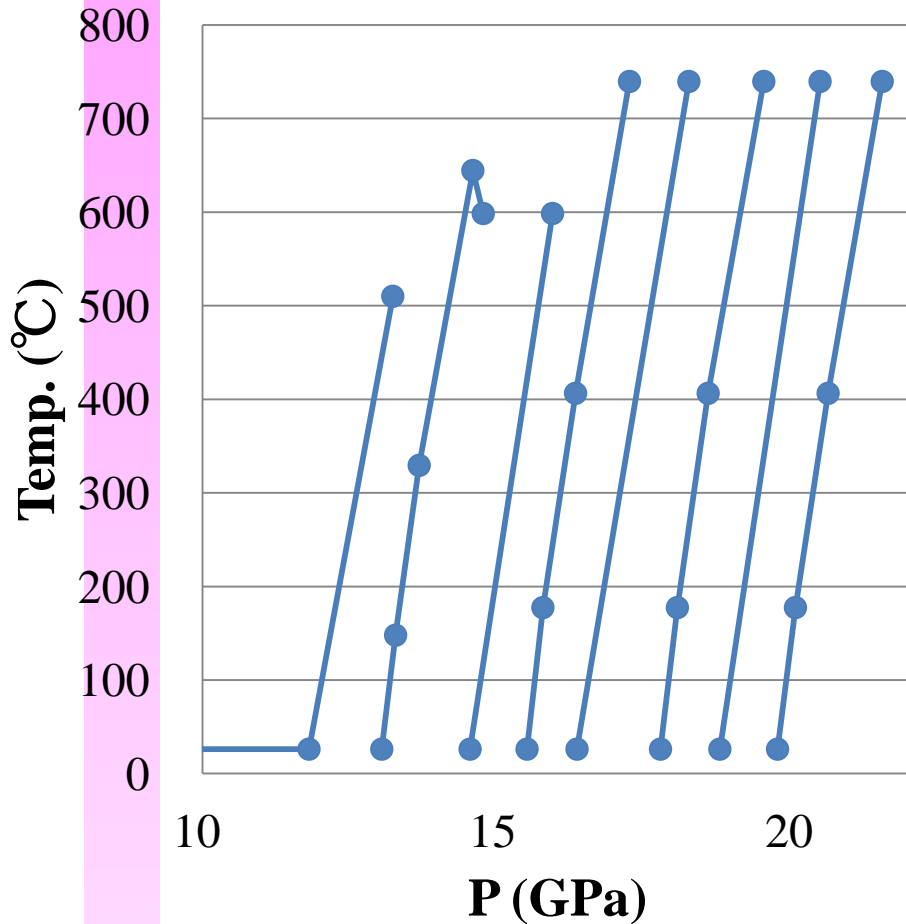
\Rightarrow **phase identification,**
lattice parameters and unit cell
volume at P,T

\Rightarrow **EoS**

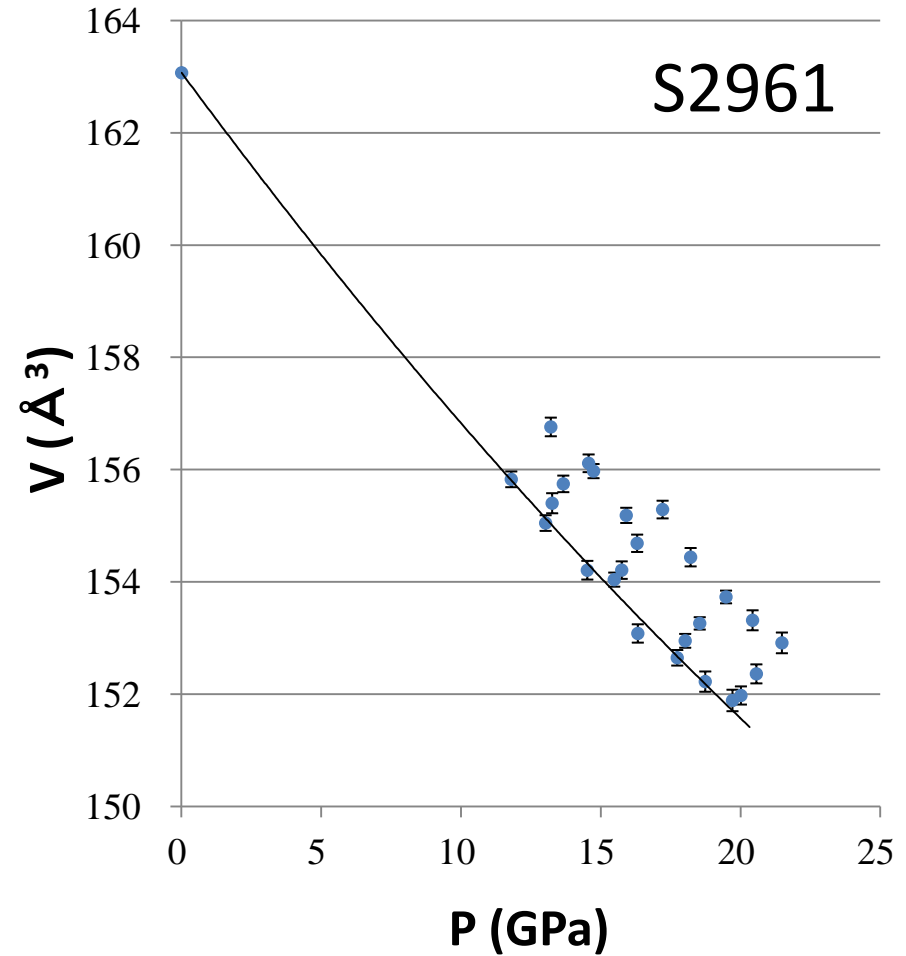


PVT of hydrous bridgmanite

Pressure-Temperature path

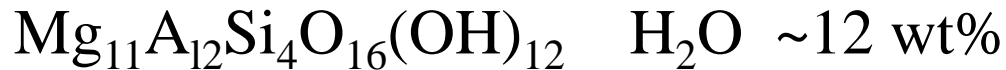


Pressure-Volume



Summary

- 1) New Al-bearing hydrous phase (23 Å phase) was found in chlorite composition in upper mantle condition. This structure is very unique, which shows elongated structure to c-direction.



Hexagonal $a=5.1972(9) \text{ \AA}$, $c=22.991(4) \text{ \AA}$

- 2) Al-bearing hydrous bridgmanite was found, which formula is $\sim \text{MgSi}_{0.9}\text{Al}_{0.1}\text{O}_3\text{H}_{0.1}$ $\text{H}_2\text{O} \sim 0.8 \text{ wt\%}$

The lattice parameters and unit cell volume were larger than those of dry bridgmanite

- 3) The crystal structure was investigated by single crystal X-ray and powder neutron diffraction methods. These show that Al prefer B-site, and hydrogen position between O2-O2 which is c-direction could be the strong candidate.

- 4) The elastic velocity measurement was conducted. The preliminary analysis shows that bulk modulus, V_p and V_s are lower than those of dry bridgmanite.

Future plan

- 1) Determination of hydrogen position precisely.
Then investigation of the effect of pressure
- 2) Determination of elastic wave velocity precisely, especially under high temperature.
- 3) Determination of EoS precisely,
- 4) The effect of pressure in the maximum water solubility in perovskite.
- 5) Investigation of the effect of Fe³⁺.

Thank you for your attention.